Trps1 activates a network of secreted Wnt inhibitors and transcription factors crucial to vibrissa follicle morphogenesis

Katherine A. Fantauzzo and Angela M. Christiano*

SUMMARY

Mutations in *TRPS1* cause trichorhinophalangeal syndrome types I and III, which are characterized by sparse scalp hair in addition to craniofacial and skeletal abnormalities. Trps1 is a vertebrate transcription factor that contains nine zinc-finger domains, including a GATA-type zinc finger through which it binds DNA. Mice in which the GATA domain of Trps1 has been deleted ($Trps1^{\Delta gt/\Delta gt}$) have a reduced number of pelage follicles and lack vibrissae follicles postnatally. To identify the transcriptional targets of Trps1 in the developing vibrissa follicle, we performed microarray hybridization analysis, comparing expression patterns in the whisker pads of wild-type versus $Trps1^{\Delta gt/\Delta gt}$ embryos. We identified a number of transcription factors and Wnt inhibitors among transcripts downregulated in the mutant embryos and several extracellular matrix proteins that were upregulated in the mutant samples, and demonstrated that target gene expression levels were altered in vivo in $Trps1^{\Delta gt/\Delta gt}$ vibrissae. Unexpectedly, we discovered that Trps1 can directly bind the promoters of its target genes to activate transcription, expanding upon its established role as a transcriptional repressor. Our findings identify Trps1 as a novel regulator of the Wnt signaling pathway and of early hair follicle progenitors in the developing vibrissa follicle.

KEY WORDS: Trps1, Hair follicle, Vibrissa, Mouse, Wnt, Extracellular matrix

INTRODUCTION

The family of trichorhinophalangeal syndromes (TRPS I, OMIM 190350; TRPS II, OMIM 150230; TRPS III, OMIM 190351) is characterized by sparse and slow-growing scalp hair, as well as craniofacial and skeletal abnormalities (Giedion et al., 1973). Heterozygous germline mutations in *TRPS1* on chromosome 8q23 result in autosomal dominant inheritance of TRPS types I and III (Momeni et al., 2000; Ludecke et al., 2001). *TRPS1* encodes a vertebrate protein with nine zinc-finger domains, including a GATA-type zinc finger and two C-terminal Ikaros-like zinc fingers (Momeni et al., 2000).

Monoallelic nonsense, missense or in-frame splice site mutations in *TRPS1*, as well as disruption or complete deletion of the gene, have been reported in cases of TRPS I (Momeni et al., 2000; Ludecke et al., 2001; Seitz et al., 2001; Hilton et al., 2002; Kaiser et al., 2004; Rossi et al., 2007; Piccione et al., 2009). Alternatively, missense mutations in exon 6 that alter the GATA-type zinc-finger domain were reported in patients classified as having the more severe TRPS III (Ludecke et al., 2001; Kobayashi et al., 2002; Hilton et al., 2002; Piccione et al., 2009). Ludecke et al. proposed that the mutant proteins resulting from these missense mutations have a decreased affinity to DNA and act in a dominant-negative manner in multiprotein complexes (Ludecke et al., 2001).

Electrophoretic mobility shift assays have demonstrated that both human and murine TRPS1 specifically bind the consensus GATA sequence (WGATAR) in DNA (Chang, G. T. et al., 2002; Malik et al., 2001). Furthermore, murine Trps1 has been shown to function as a sequence-specific transcriptional repressor in both reporter gene assays and *Xenopus* embryo explant experiments,

with the ability to repress GATA-dependent activation in a dose-dependent manner (Malik et al., 2001). This repression was dependent on the integrity of the Trps1 GATA-type zinc-finger domain and also required the C-terminal 119 amino acids of the protein, which harbor the two Ikaros-like zinc-finger domains (Malik et al., 2001). Consistent with their crucial role in mediating the transcriptional activity of Trps1, the sequences of the GATA-type zinc-finger motif and the neighboring basic regions, as well as the Ikaros-type zinc fingers, are 100% conserved at the amino acid level between *Xenopus*, mouse and human TRPS1 proteins (Malik et al., 2001).

TRPS1 has been shown to transcriptionally repress five target genes through specific binding to consensus GATA sites in their promoters, four of which are expressed in bone. These transcriptional targets include prostate-specific antigen (*PSA*; also known as *KLK3*) (van den Bemd et al., 2003), runt-related transcription factor 2 (*RUNX2*) (Napierala et al., 2005), signal transducer and activator of transcription 3 (*Stat3*) (Suemoto et al., 2007), parathyroid hormone-related protein (*Pthrp*; also known as *Pthlh*) (Nishioka et al., 2008) and osteocalcin (*BGLAP*) (Piscopo et al., 2009). In each case, mutation of the consensus GATA binding sites abolished TRPS1-mediated repression of target gene transcription.

To investigate the role of Trps1 during mammalian development, Malik et al. generated mice with a targeted in-frame deletion of the GATA-type zinc-finger domain (Malik et al., 2002). The resulting $Trps1^{\Delta gt/\Delta gt}$ mice displayed a number of hair follicle, craniofacial and skeletal defects that mirror the phenotypic characteristics of human TRPS patients. Homozygous $Trps1^{\Delta gt/\Delta gt}$ mice died within 6 hours of birth due to respiratory failure stemming from thoracic skeletal defects. Homozygous mutant mice were further reported to completely lack vibrissae follicles during late gestation, with no histological evidence of earlier follicle formation. In addition, neonatal $Trps1^{\Delta gt/\Delta gt}$ mice exhibited a ~50% reduction in dorsal pelage follicle density compared with their wild-type littermates (Malik et al., 2002). More recently, $Trps1^{-/-}$ mice were generated and reported to display 'severe hair follicle abnormalities' without

Department of Dermatology and Department of Genetics and Development, Columbia University, New York, NY 10032, USA.

*Author for correspondence (amc65@columbia.edu)

further elaboration (Suemoto et al., 2007). While these studies revealed that Trps1 is necessary for proper hair follicle formation, they did not address the molecular mechanisms by which Trps1 regulates hair follicle development.

Here, we performed a detailed histological analysis of early vibrissa follicle development in $Trps1^{\Delta gt/\Delta gt}$ mouse embryos, revealing mutant vibrissae hair germs that were reduced in number, irregularly spaced and markedly smaller than those of their wild-type counterparts. To gain insight into the role of Trps1 as a transcriptional regulator in the hair follicle, we performed microarray hybridization analysis, comparing expression patterns in whole whisker pads of wild-type versus $Trps1^{\Delta gt/\Delta gt}$ embryos. Our findings uncovered a network of transcription factors, Wnt inhibitors and extracellular matrix proteins regulated by Trps1 during early vibrissa follicle morphogenesis and demonstrated, for the first time, that Trps1 is capable of acting as a transcriptional activator.

MATERIALS AND METHODS

Mice
$Trps1^{+/tm1Shiv}$ mice (Malik et al., 2002), which are referred to in the text as $Trps1^{+/\Delta gt}$, were a gift of Dr R. Shivdasani (Dana-Farber Cancer Institute at Harvard Medical School). All mouse experiments were performed under approval of the Institutional Animal Care and Use Committee of Columbia University.

Histology
Whole muzzle skin dissected from embryonic day (E) 12.5-13.5 embryos (day of plug considered E0.5) was dissected in PBS, fixed in 10% formalin for up to 72 hours, washed through an ethanol series and embedded in paraffin. After deparaffinization and rehydration, sections (8 μm) were stained with Hematoxylin and Eosin and permanently mounted with Permount (Thermo Fisher Scientific, Waltham, MA, USA). Sections were photographed using an HRc AxioCam fitted onto an Axioplan2 fluorescence microscope (Carl Zeiss, Thornwood, NY, USA). Vibrissa follicle quantifications were performed using the measurement tool in AxioVision 4.5 software (Carl Zeiss).

Immunofluorescence analysis
Whole muzzle skin dissected at multiple timepoints from E12.5 to postnatal day (P) 1 was mounted in O.C.T. compound (Sakura Finetek, Torrance, CA, USA) and frozen in liquid nitrogen. Sections (8 μm) were fixed in 4% paraformaldehyde (PFA)/0.1% Triton X-100 for 10 minutes at room temperature or in methanol for 15 minutes at –20°C followed by acetone for 2 minutes at –20°C and washed in PBS. Sections were blocked for 1 hour in 10% heat-inactivated goat or donkey serum in PBS and incubated overnight at 4°C in primary antibody diluted in 1% serum in PBS. Primary antibodies and dilutions were as follows: anti-Trps1 [1:5000; gift of Dr R. Shivdasani (Malik et al., 2001)]; anti-P-cadherin (1:100; Invitrogen, Carlsbad, CA, USA); anti-syndecan 1 (1:200; BD Pharmingen, San Jose, CA, USA); anti-Lhx2 (1:10,000; gift of Dr T. Jessell, Columbia University, New York); anti-Tnc (1:200; Sigma-Aldrich, St Louis, MO, USA); and anti-Lef1 (1:25; Cell Signaling Technology, Danvers, MA, USA). After washing in PBS, sections were incubated in either an Alexa Fluor 594 donkey anti-rat IgG, Alexa Fluor 488 goat anti-rabbit IgG or Alexa Fluor 594 goat anti-rabbit IgG (Molecular Probes, Invitrogen) secondary antibody (1:500) diluted in 1% serum in PBS for 1 hour. Sections were mounted in VECTASHIELD mounting medium with DAPI (Vector Laboratories, Burlingame, CA, USA) and photographed using an HRc AxioCam fitted onto an Axioplan2 fluorescence microscope or an LSM 5 laser-scanning Axio Observer Z1 confocal microscope (Carl Zeiss).

Microarray hybridization analysis
Whole whisker pads were dissected from E12.5 embryos and total RNA was isolated using the RNeasy Mini Kit (Qiagen, Valencia, CA, USA) according to the manufacturer's instructions. Triplicate RNA samples from three independent embryos of each genotype were amplified and labeled for hybridization to Affymetrix GeneChip MOE430A microarrays using Affymetrix reagents and protocols (Affymetrix, Santa Clara, CA, USA). The data output was analyzed using GeneSpring GX 10.0 software (Agilent Technologies, Palo Alto, CA, USA). P-values were calculated using an unpaired t-test. Expression values with $P \leq 0.05$ and a fold difference of at least 1.5 relative to wild-type baseline expression levels were considered significant. Microarray data have been deposited at the Gene Expression Omnibus with the Accession Number GSE33766.

Quantitative (q) RT-PCR
First-strand cDNA was synthesized from total RNA isolated from whole muzzle skin dissected from E12.5 embryos using a 2:1 ratio of random primers to oligo(dT) primer and SuperScript III reverse transcriptase (Invitrogen) according to the manufacturer's instructions. qRT-PCR was performed on an ABI 7300 machine and analyzed with ABI Relative Quantification Study software (Applied Biosystems, Foster City, CA, USA). Primers were designed according to ABI guidelines and all reactions were performed using Power SYBR Green PCR Master Mix (Applied Biosystems), 250 nM primers (Invitrogen) and 100 ng cDNA in a 20 μl reaction volume. The following PCR protocol was used: step 1, 50°C 2 minutes; step 2, 95°C 10 minutes; step 3, 95°C 15 seconds; step 4, 60°C 1 minute; repeat steps 3 and 4 for 40 cycles. All samples were run in quadruplicate for three independent runs and normalized against an endogenous internal control, $B2m$. PCR products were electrophoresed on a 1% agarose TBE gel containing ethidium bromide and photographed with an Electrophoresis Documentation and Analysis System 120 camera (Kodak, Rochester, NY, USA) to confirm amplicon size. qRT-PCR primers are listed in supplementary material Table S1.

Immunohistochemistry
Immunohistochemistry was performed on sections (8 μm) of paraffin-embedded whole muzzle skin dissected from E16.5 embryos using an anti-Prdm1 mouse monoclonal antibody (gift of Dr K. Calame, Columbia University, New York) based on a previously published protocol (Chang, D. H. et al., 2002). Sections were photographed using an HRc AxioCam fitted onto an Axioplan2 fluorescence microscope (Carl Zeiss).

In situ hybridization
An 852 bp probe template spanning from exon 2 to the 3′ UTR of $Sox18$ was amplified by PCR from an E15.0 dermal cDNA stock using the following primers: mSox18-F, 5′-CGCGACCATCCCAACTACAAGTAC-3′; and mSox18-R, 5′-AAAGATGCCATTTCTGTCGCCTCC-3′. The PCR product was cloned into the pCRII dual promoter (T7 and SP6) vector (Invitrogen) and standard procedures were followed for the preparation of digoxigenin-labeled cRNA (Roche Applied Science, Indianapolis, IN, USA) antisense and control sense probes. We previously reported the $Apcdd1$ (Shimomura et al., 2010) and $Dkk4$ (Bazzi et al., 2007) probes. In situ hybridization was performed on sections (16 μm) of sucrose-infiltrated frozen whole muzzle skin dissected from E12.5 embryos based on our previously published protocol (Shimomura et al., 2010). Sections were photographed using an HRc AxioCam fitted onto an Axioplan2 fluorescence microscope (Carl Zeiss).

Functional annotation analysis
The list of transcripts generated by microarray hybridization analysis was analyzed using the Babelomics 4.2.0 suite (http://babelomics.bioinfo.cipf.es). Single enrichment analysis was performed with the FatiGO tool, using a two-tailed Fisher's exact test to identify over-represented functional annotations in the transcript list compared with the entire genome. Results with $P < 0.05$ were considered significant.

Chromatin immunoprecipitation (ChIP)
HEK 293T cells were seeded onto 10 cm dishes and cultured to 80-90% confluency in Dulbecco's Modified Eagle's Medium (Gibco, Invitrogen) supplemented with 10% fetal bovine serum (FBS) (Gibco), 100 IU/ml penicillin and 100 μg/ml streptomycin (P/S). The cells were treated with 1% formaldehyde for 10 minutes at 37°C, washed twice with cold PBS containing protease inhibitors and harvested. ChIP was carried out using the Chromatin Immunoprecipitation Assay Kit (Millipore, Billerica, MA, USA) according to the manufacturer's instructions. Cell lysates were precipitated

with 3 µg of anti-Trps1 rabbit polyclonal antibody (gift of Dr R. Shivdasani) or normal rabbit IgG (Santa Cruz Biotechnology, Santa Cruz, CA, USA) as a negative control. After elution, DNA was recovered using the Rapid PCR Purification System (Marligen Biosciences, Ijamsville, MD, USA). PCR reactions were performed using input, IgG-precipitated and Trps1-precipitated DNA samples, Platinum PCR SuperMix (Invitrogen) and 0.67 µM primers (Invitrogen) in a 30 µl reaction volume. The following PCR protocol was used: step 1, 94°C 5 minutes; step 2, 94°C 45 seconds; step 3, 55°C 30 seconds; step 4, 72°C 1 minute; repeat steps 2-4 for 36-40 cycles; step 5, 72°C 10 minutes. PCR products were electrophoresed on a 1% agarose TBE gel containing ethidium bromide and photographed with an Electrophoresis Documentation and Analysis System 120 camera (Kodak). Positive immunoprecipitation results were confirmed in at least two independent trials. PCR primers are listed in supplementary material Table S1.

Promoter assays
The *Sox18* promoter (2510 bp upstream of the translation initiation site) was amplified by PCR from a C57BL/6 DNA stock using the following primers: mSox18p-F-XhoI, 5′-CAACTCGAGCTCACTTTGGCCAAA-GCTAG-3′; and mSox18p-R-HindIII, 5′-GACAAGCTTGATCTCT-GCATTCCAGCTC-3′. The amplified product was subcloned into the *Xho*I and *Hin*dIII sites of the luciferase reporter vector pGL3-Basic (Promega, Madison, WI, USA). We previously reported the *Dkk4* promoter construct (Bazzi et al., 2007).

Saos-2 cells were seeded onto 6-well dishes 24 hours before transfection. At 80-90% confluency, a mouse Trps1 expression plasmid or pCXN2.1 backbone vector (1 µg) were transfected into each well in combination with the mouse *Sox18* promoter reporter plasmid, mouse *Dkk4* promoter reporter plasmid or pGL3 backbone vector (1 µg) using FuGENE HD (Roche Applied Science). A plasmid encoding a β-galactosidase reporter (0.5 µg) was also transfected for normalization of transfection efficiency. The cells were cultured for 24 hours after transfection in McCoy's 5A Medium Modified (Invitrogen) with 15% FBS and P/S, harvested and lysed. Luciferase and β-galactosidase signals were measured using the Luciferase Assay System (Promega) and β-Galactosidase Enzyme Assay System with Reporter Lysis Buffer (Promega), respectively, according to the manufacturer's instructions. All assays were performed in triplicate for three independent trials.

TOP-flash Wnt reporter assays
HEK 293T cells were seeded onto 12-well dishes 24 hours before transfection. At 80% confluency, a TOP-flash Wnt reporter plasmid (50 ng) was transfected into each well in combination with expression plasmids for human LEF1 (100 ng), human β-catenin (500 ng) (both gifts of Dr J. Kitajewski, Columbia University, New York) and/or mouse Trps1 (500 ng) using Lipofectamine 2000 (Invitrogen). A plasmid encoding a β-galactosidase reporter (100 ng) was also transfected for normalization of transfection efficiency. The cells were cultured for 36 hours after transfection in Opti-MEM (Gibco), harvested and lysed. Luciferase and β-galactosidase signals were measured as described above. All assays were performed in triplicate for three independent trials.

RESULTS
Early vibrissa follicle morphogenesis is strikingly abnormal in *Trps1*$^{\Delta gt/\Delta gt}$ mutant embryos
We began by performing histological analysis of vibrissa follicle development during the earliest stages of morphogenesis in *Trps1*$^{\Delta gt/\Delta gt}$ mouse embryos. Mutant vibrissae placodes (Fig. 1B) were reduced in number and irregularly spaced at E12.5 compared with those found in wild-type littermates (Fig. 1A). These abnormalities were even more pronounced at E13.5 (Fig. 1C,D; supplementary material Fig. S1A-C), when *Trps1*$^{\Delta gt/\Delta gt}$ vibrissae were noticeably shorter than their wild-type counterparts (Fig. 1E). Furthermore, whereas 68.00±4.90% of *Trps1*$^{+/+}$ vibrissae had reached the peg stage of morphogenesis by E13.5, the mutant vibrissae were developmentally delayed, with only 12.38±6.04% ($P<0.001$) having reached the peg stage by this timepoint (Fig. 1F).

We next compared the levels of P-cadherin and syndecan 1 between wild-type and *Trps1*$^{\Delta gt/\Delta gt}$ vibrissae to examine the relative size and location of the epithelial and mesenchymal compartments, respectively. P-cadherin was expressed throughout the follicular epithelium of both wild-type and mutant vibrissae, with highest expression levels at the leading edge of the invaginating follicles (Fig. 1G,H). Similarly, syndecan 1 staining was relatively consistent in the mesenchyme surrounding wild-type and *Trps1*$^{\Delta gt/\Delta gt}$ developing vibrissae (Fig. 1I,J).

As the development of *Trps1*$^{\Delta gt/\Delta gt}$ vibrissae is dysregulated from the earliest stages of morphogenesis, we next performed immunofluorescence analysis to examine the expression of Trps1 during vibrissa follicle induction, specifically at E12.5 when the vibrissae placodes are first discernible, in an attempt to identify the cell population(s) responsible for the mutant phenotype. Trps1 expression was intense and nuclear in the mesenchymal cells underlying the anlagen of the developing vibrissae follicles, while more diffuse in the overlying epithelial cells of the placode (Fig. 1K,L), predicting a role for this transcription factor in both compartments of the developing vibrissa.

Identification of downstream transcriptional targets of Trps1 in the whisker pad
In order to identify genes that are transcriptionally regulated by Trps1 in both the epithelium and mesenchyme of the follicle during early morphogenesis, we performed microarray hybridization analysis, comparing expression patterns in whole whisker pads of wild-type versus *Trps1*$^{\Delta gt/\Delta gt}$ embryos at E12.5. Expression values with $P \leq 0.05$ and a fold difference of at least 1.5 relative to wild-type baseline expression levels were considered significant. A box-and-whisker plot of the microarray data revealed a similar distribution of normalized intensity values across all of the samples used (supplementary material Fig. S2A), and non-biased hierarchical analysis demonstrated clustering of the biological replicates (supplementary material Fig. S2B).

A relatively short list of differentially expressed transcripts was generated (Table 1), many of which have known expression patterns in the skin or hair follicle. Eighteen transcripts were found to be downregulated in the mutant samples (supplementary material Fig. S2C). These included a number of transcription factors, such as *Prdm1*, *Sox18*, *Lhx2* and *Sox21*, among others, and secreted or membrane-bound Wnt inhibitors, including *Wif1*, *Apcdd1* and *Dkk4*. Conversely, 32 transcripts were found to be upregulated in the mutant samples (supplementary material Fig. S2C), many of which encode extracellular matrix proteins, including *Epyc*, *Dcn*, *Lum* and *Tnc*.

We validated the expression changes of selected transcripts by quantitative real-time PCR (qRT-PCR) analysis and found that the transcriptional trends were upheld, with a significant change ($P<0.05$) in target gene expression levels in the *Trps1*$^{\Delta gt/\Delta gt}$ samples (Fig. 2).

Trps1 target gene expression levels are altered in vivo in *Trps1*$^{\Delta gt/\Delta gt}$ vibrissae follicles
Beginning with transcripts in the upper portion of the list which we hypothesized are activated (directly or indirectly) by Trps1, we next compared the expression of a subset of these potential Trps1 target genes between wild-type and *Trps1*$^{\Delta gt/\Delta gt}$ embryos in vivo. Immunohistochemistry performed on E16.5 whisker pads revealed decreased Prdm1 expression in the dermal papillae and inner root sheath precursors of *Trps1*$^{\Delta gt/\Delta gt}$ vibrissae follicles (Fig. 3A,B). In situ hybridization analysis on E12.5 whisker pads demonstrated
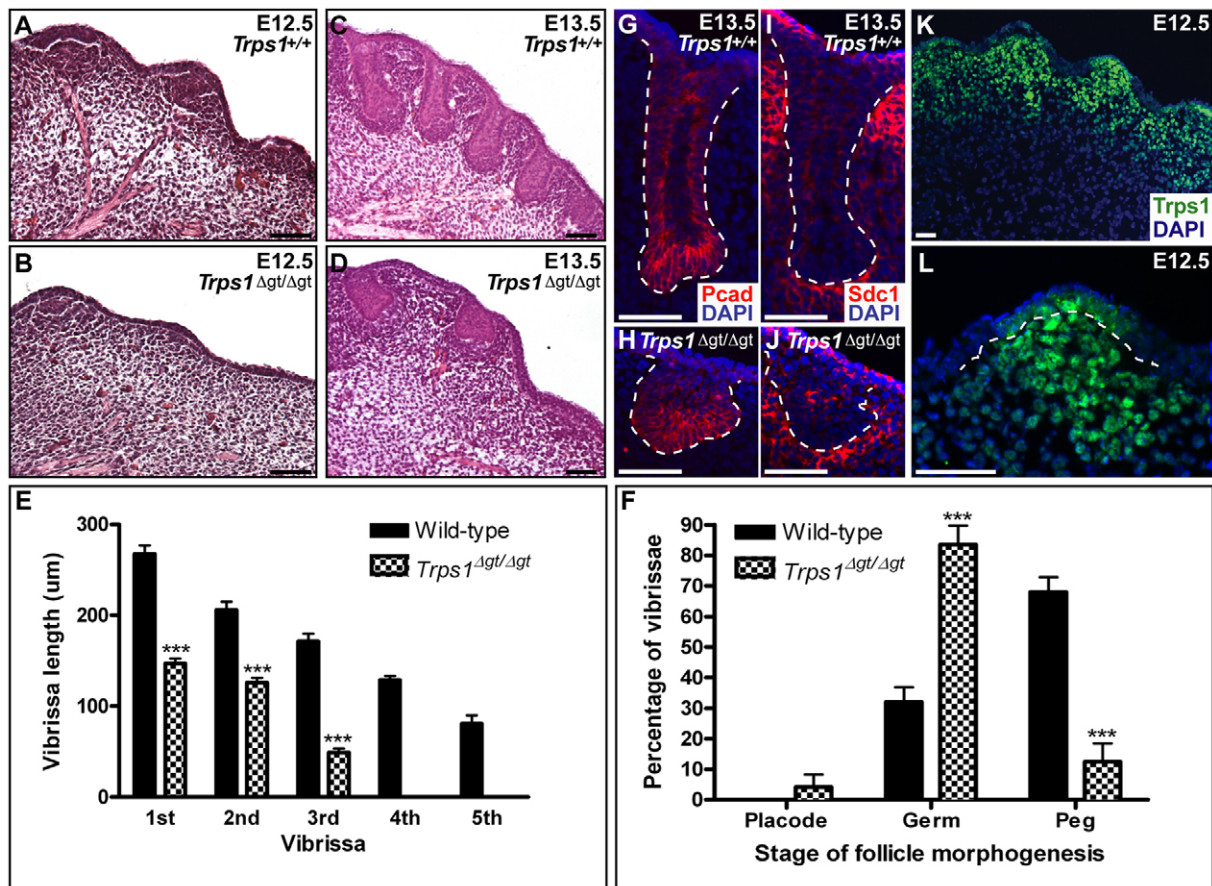
Fig. 1. Early morphogenesis vibrissa follicle abnormalities in *Trps1*^{Δgt/Δgt} mutant mouse embryos. (**A**,**B**) Hematoxylin and Eosin staining of transverse *Trps1*^{+/+} (A) and *Trps1*^{Δgt/Δgt} (B) whisker pad sections at E12.5 revealed a reduced number of vibrissae placodes, which were irregularly spaced in mutant embryos. (**C**,**D**) Hematoxylin and Eosin staining of transverse *Trps1*^{+/+} (C) and *Trps1*^{Δgt/Δgt} (D) whisker pad sections at E13.5 revealed short, developmentally delayed vibrissae follicles in mutant embryos. (**E**) Row E vibrissa follicle length in *Trps1*^{+/+} versus *Trps1*^{Δgt/Δgt} E13.5 embryos. (**F**) The percentage of row E vibrissae at each stage of follicle morphogenesis in *Trps1*^{+/+} versus *Trps1*^{Δgt/Δgt} E13.5 embryos. Statistical analyses were performed using a two-tailed unpaired *t*-test. Data are presented as mean±s.e.m. ***, $P<0.001$. (**G**,**H**) P-cadherin staining (red) was consistent in the follicular epithelium of *Trps1*^{+/+} (G) and *Trps1*^{Δgt/Δgt} (H) vibrissae at E13.5. (**I**,**J**) Syndecan 1 staining (red) was similar in the mesenchyme surrounding developing *Trps1*^{+/+} (I) and *Trps1*^{Δgt/Δgt} (J) vibrissae at E13.5. (**K**,**L**) Trps1 staining (green) was intense and nuclear in the mesenchymal cells underlying the anlagen of developing vibrissae and more diffuse in the overlying epithelial cells of the placode at E12.5. Nuclei were stained with DAPI (blue). Scale bars: 100 μm.

decreased *Sox18* expression in the dermal condensates underlying the developing vibrissae placodes in *Trps1*^{Δgt/Δgt} embryos (Fig. 3C,D). Furthermore, immunofluorescence analysis performed on E12.5 whisker pads revealed decreased Lhx2 expression throughout the epithelial placodes of *Trps1*^{Δgt/Δgt} vibrissae, particularly in the basal layer (Fig. 3E,F). These in vivo expression differences were all consistent with the trends predicted by the microarray hybridization analysis.

As characterization of Lhx2 protein expression in the hair follicle had thus far been described only for pelage hairs (Rhee et al., 2006; Törnqvist et al., 2010), we performed immunofluorescence analysis of the expression of Lhx2 during vibrissa follicle morphogenesis. Compared with its expression in the developing pelage follicle, we found expansion of the Lhx2 expression domain into additional layers of the follicular epithelium, in particular the inner root sheath layers (supplementary material Fig. S3). Furthermore, we detected faint Lhx2 expression in the dermal papilla as early as E14.5, as well as in the dermal cells of the vibrissae-specific collagen capsule surrounding the developing follicles (supplementary material Fig. S3). Importantly, this pattern of Lhx2 expression overlapped with that reported for Trps1 in developing vibrissae (Fantauzzo et al., 2008b).

Trps1 globally represses the expression of extracellular matrix proteins in the whisker pad

Next, we focused on the lower portion of the microarray list and performed single enrichment analysis using the Babelomics 4 suite to identify over-represented functional annotations compared with the genome as a whole. Proteinaceous extracellular matrix (GO:0005578) was the most significant GO term detected in the cellular component analysis, with an adjusted *P*-value of $9.96×10^{-7}$. Transcripts within our list associated with this term included *Epyc*, *Egr1*, *Dcn*, *Lum*, *Tnc*, *Col8a1*, *Fus* and *Tinag* (supplementary material Fig. S4).

Immunofluorescence analysis of one of these extracellular matrix proteins, Tnc, revealed striking increases in expression in the mesenchyme underlying developing *Trps1*^{Δgt/Δgt} vibrissae follicles at E12.5 and E13.5 (Fig. 3G-J). Our findings thus

Table 1. Transcripts differentially expressed between *Trps1*+/+ and *Trps1*Δgt/Δgt E12.5 mouse whisker pad samples as detected by microarray hybridization analysis

| Gene	Symbol	Fold change
poly(A) binding protein interacting protein 1	Paip1	4.5
Wnt inhibitory factor 1	Wif1	2.4
PR domain containing 1, with ZNF domain	Prdm1	2.1
SRY-box containing gene 18	Sox18	2.0
LIM homeobox protein 2	Lhx2	1.9
galactosylceramidase	Galc	1.7
dual specificity phosphatase 9	Dusp9	1.7
polyribonucleotide nucleotidyltransferase 1	Pnpt1	1.7
adenomatosis polyposis coli down-regulated 1	Apcdd1	1.7
solute carrier family 4, member 1	Slc4a1	1.7
dickkopf homolog 4	Dkk4	1.7
SRY-box containing gene 21	Sox21	1.6
cyclin-dependent kinase inhibitor 1A	Cdkn1a	1.6
peripheral myelin protein 22	Pmp22	1.6
nephroblastoma overexpressed gene	Nov	1.5
zinc finger protein 213	Zfp213	1.5
methylcrotonoyl-coenzyme A carboxylase 1	Mccc1	1.5
CD59a antigen	Cd59a	1.5
tubulointerstitial nephritis antigen	Tinag	−1.5
Kruppel-like factor 6	Klf6	−1.5
LPS-responsive beige-like anchor	Lrba	−1.5
gamma-aminobutyric acid (GABA-A) receptor; subunit beta 1	Gabrb1	−1.5
brain derived neurotrophic factor	Bdnf	−1.5
kinesin light chain 1	Klc1	−1.5
syndecan 4	Sdc4	−1.5
fusion; derived from t(12;16) malignant liposarcoma (human)	Fus	−1.6
potassium channel tetramerisation domain containing 12	Kctd12	−1.6
splicing factor; arginine/serine-rich 7	Sfrs7	−1.6
glutamyl aminopeptidase	Enpep	−1.6
LUC7-like 2 (S. cerevisiae)	Luc7l2	−1.6
trichorhinophalangeal syndrome I (human)	Trps1	−1.7
collagen; type VIII; alpha 1	Col8a1	−1.7
stathmin-like 2	Stmn2	−1.7
protein tyrosine phosphatase; receptor type; D	Ptprd	−1.7
transmembrane channel-like gene family 4	Tmc4	−1.7
tenascin C	Tnc	−1.8
lumican	Lum	−1.8
DEAH (Asp-Glu-Ala-His) box polypeptide 30	Dhx30	−1.8
thymus cell antigen 1; theta	Thy1	−1.8
trans-acting transcription factor 5	Sp5	−1.8
enhancer of yellow 2 homolog (Drosophila)	Eny2	−1.9
serine (or cysteine) peptidase inhibitor; clade C (antithrombin); member 1	Serpinc1	−1.9
decorin	Dcn	−1.9
early growth response 1	Egr1	−2.0
interferon inducible GTPase 1	Iigp1	−2.0
calcitonin/calcitonin-related polypeptide; alpha	Calca	−2.3
calbindin-28K	Calb1	−2.3
tyrosine 3-monooxygenase/tryptophan 5-monooxygenase activation protein; zeta polypeptide	Ywhaz	−2.4
epiphycan	Epyc	−3.1
FBJ osteosarcoma oncogene	Fos	−3.1

Fold changes are relative to wild-type expression levels.

demonstrate that Trps1 regulates the expression of extracellular matrix proteins throughout the whisker pad microenvironment, in addition to its role as a transcriptional regulator within the developing vibrissa follicle.

Trps1 directly binds the promoters of its target genes to activate transcription

To determine whether Trps1 directly binds the promoters of the potential target genes identified by microarray hybridization analysis in this study, we located consensus GATA-binding sites within 3 kb of the transcriptional start site of the human *WIF1*,

PRDM1, *SOX18*, *LHX2*, *APCDD1*, *DKK4* and *SOX21* promoters and performed endogenous chromatin immunoprecipitation (ChIP) experiments in HEK 293T cells. We found that Trps1 bound up to ten sites in the *WIF1* promoter out of 15 potential binding sites in the DNA. Similarly, Trps1 bound one site each in the *SOX18* and *LHX2* promoters, up to four sites each in the *APCDD1* and *DKK4* promoters, and up to three sites in the *SOX21* promoter (Fig. 4A). Despite the presence of two consensus GATA-binding sites within 3 kb of the transcriptional start site of *PRDM1*, Trps1 binding was never observed in this promoter (data not shown), indicating that Trps1 regulates *PRDM1* expression in an indirect manner.
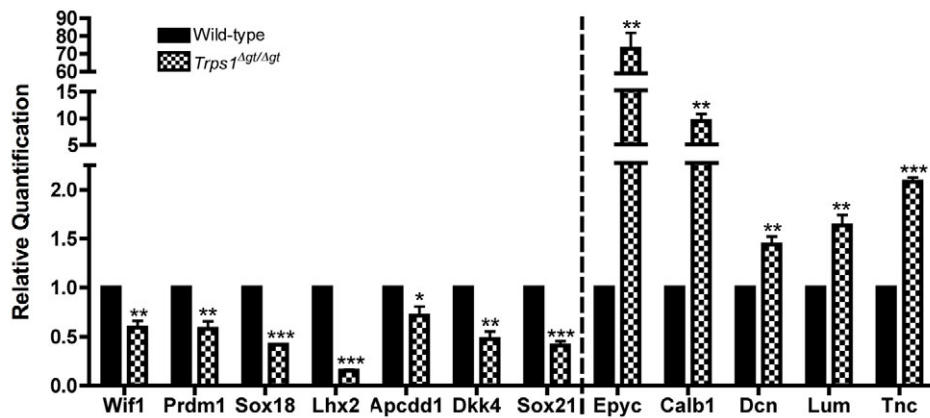
Fig. 2. Validation of downstream transcriptional targets of Trps1 in the whisker pad. qRT-PCR values validating the trends of representative transcript expression between $Trps1^{+/+}$ and $Trps1^{\Delta gt/\Delta gt}$ E12.5 whisker pad samples. Statistical analyses were performed using a two-tailed unpaired t-test. Data are presented as mean±s.e.m. *, $P<0.05$; **, $P<0.01$; ***, $P<0.001$.

To date, the prevailing view asserts that Trps1 acts exclusively as a transcriptional repressor in various contexts (van den Bemd et al., 2003; Napierala et al., 2005; Suemoto et al., 2007; Nishioka et al., 2008; Piscopo et al., 2009). In light of our in vivo expression and ChIP results, we revisited this notion and postulated that Trps1 can also function as a transcriptional activator. We performed luciferase reporter promoter assays in the human epithelial osteosarcoma cell line Saos-2 and demonstrated that Trps1 activated both *Sox18* (30.13±15.88%; $P=0.0759$) and *Dkk4* (28.09±11.32%; $P=0.0254$) transcription (Fig. 4B). These results reveal a novel role for Trps1 as a direct transcriptional activator of downstream target genes.

Wnt expression is upregulated in $Trps1^{\Delta gt/\Delta gt}$ vibrissae follicles

Notably, three Wnt inhibitors, *Wif1*, *Apcdd1* and *Dkk4*, were detected among the transcripts downregulated in the $Trps1^{\Delta gt/\Delta gt}$ whisker pad samples by microarray hybridization analysis, leading us to postulate that Trps1 may repress the Wnt signaling pathway. In situ hybridization analysis at E12.5 revealed that *Apcdd1* expression was decreased in both the epithelial placode and underlying mesenchyme of $Trps1^{\Delta gt/\Delta gt}$ vibrissae (Fig. 5A,B), and that *Dkk4* expression was decreased throughout the epithelial placodes of the developing mutant vibrissae and the surrounding interfollicular whisker pad epidermis (Fig. 5C,D).

To examine whether the decreased expression of these Wnt inhibitors in $Trps1^{\Delta gt/\Delta gt}$ vibrissae led to a concomitant increase in canonical Wnt signaling in these follicles, we examined the expression of Lef1 by immunofluorescence analysis. Whereas Lef1 was strongly expressed in the nuclei of mesenchymal cells in both the wild-type and $Trps1^{\Delta gt/\Delta gt}$ whisker pad dermis, its expression was markedly increased in the epithelial cells of the placode in the mutant follicles (Fig. 5E,F).

To further define the effect of Trps1 expression on canonical Wnt signaling, we performed a series of Wnt reporter assays in HEK 293T cells using the TCF/LEF luciferase reporter plasmid TOP-flash. As expected, TOP-flash activity was modestly increased over baseline levels with the addition of either LEF1 or β-catenin, and dramatically increased in the presence of both proteins (Fig. 5G). The addition of Trps1 significantly repressed (53.81±5.30%; $P<0.001$) the LEF1- and β-catenin-mediated activation of TOP-flash activity (Fig. 5G). Taken together, these findings identify Trps1 as a novel regulator of the canonical Wnt signaling pathway through its direct activation of several Wnt inhibitors.

DISCUSSION

In this study, we identified a number of downstream transcriptional targets of Trps1, including several Wnt inhibitors and extracellular matrix proteins. Moreover, we demonstrated that Trps1 upregulates the expression of multiple transcription factors in the vibrissa follicle, including *Prdm1*, *Sox18*, *Lhx2* and *Sox21*, and, furthermore, that Trps1 directly binds the promoters of all but the first of these target genes to activate their transcription. These data establish a crucial role for Trps1 as an upstream regulator of transcriptional hierarchies in both compartments of the hair follicle. Importantly, we demonstrate, for the first time, the ability of Trps1 to function as a transcriptional activator, expanding upon its reported role as a transcriptional repressor.

Each of the transcription factors identified as targets of Trps1 in this microarray study have expression domains that colocalize in vivo with Trps1 in at least one compartment of the skin or hair follicle (Fantauzzo et al., 2008a) (Table 2). Notably, $Trps1^{\Delta gt/\Delta gt}$ mice share phenotypic similarities with mutant mouse models of many of these transcription factors (Table 2). For instance, late gestation embryos with epiblast-specific deletion of the gene encoding the Krüppel-type zinc-finger transcription factor Prdm1 ($Sox2-Cre;Prdm1^{BEH/fl}$) lack vibrissae follicles completely (Robertson et al., 2007), which is comparable to the absence of vibrissae follicles observed at birth in $Trps1^{\Delta gt/\Delta gt}$ mice. Moreover, embryos null for the LIM homeobox transcription factor Lhx2 ($Lhx2^{-/-}$) display a ~40% reduction in pelage follicle density (Rhee et al., 2006), analogous to the reduced pelage follicle density in $Trps1^{\Delta gt/\Delta gt}$ embryos.

Two members of the SRY box-containing family of transcription factors, *Sox18* and *Sox21*, were also identified as targets of Trps1 in this study and both have corresponding mutant mouse models that display vibrissae follicle defects. Point mutations in *Sox18* have been shown to underlie the ragged (*Ra*) mouse phenotype, which is characterized by varying degrees of coat sparseness (Pennisi et al., 2000a). $Sox18^{Ra/+}$ heterozygous neonates have short vibrissae and a thin, ragged pelage coat that lacks secondary auchene and zigzag hairs, whereas homozygous mutants almost completely lack vibrissae and coat hairs (Carter and Phillips, 1954). This vibrissa follicle phenotype is consistent with that observed in $Trps1^{\Delta gt/\Delta gt}$ mice, while the pelage coat defect is more severe. In humans, mutations in *SOX18* result in hypotrichosis-lymphedema-telangiectasia syndrome (OMIM 607823), which is typified by an absence of eyebrows and eyelashes, and by sparse scalp hair (Irrthum et al., 2003) reminiscent of the scalp hypotrichosis found in patients with TRPS types I and III (Giedion et al., 1973).
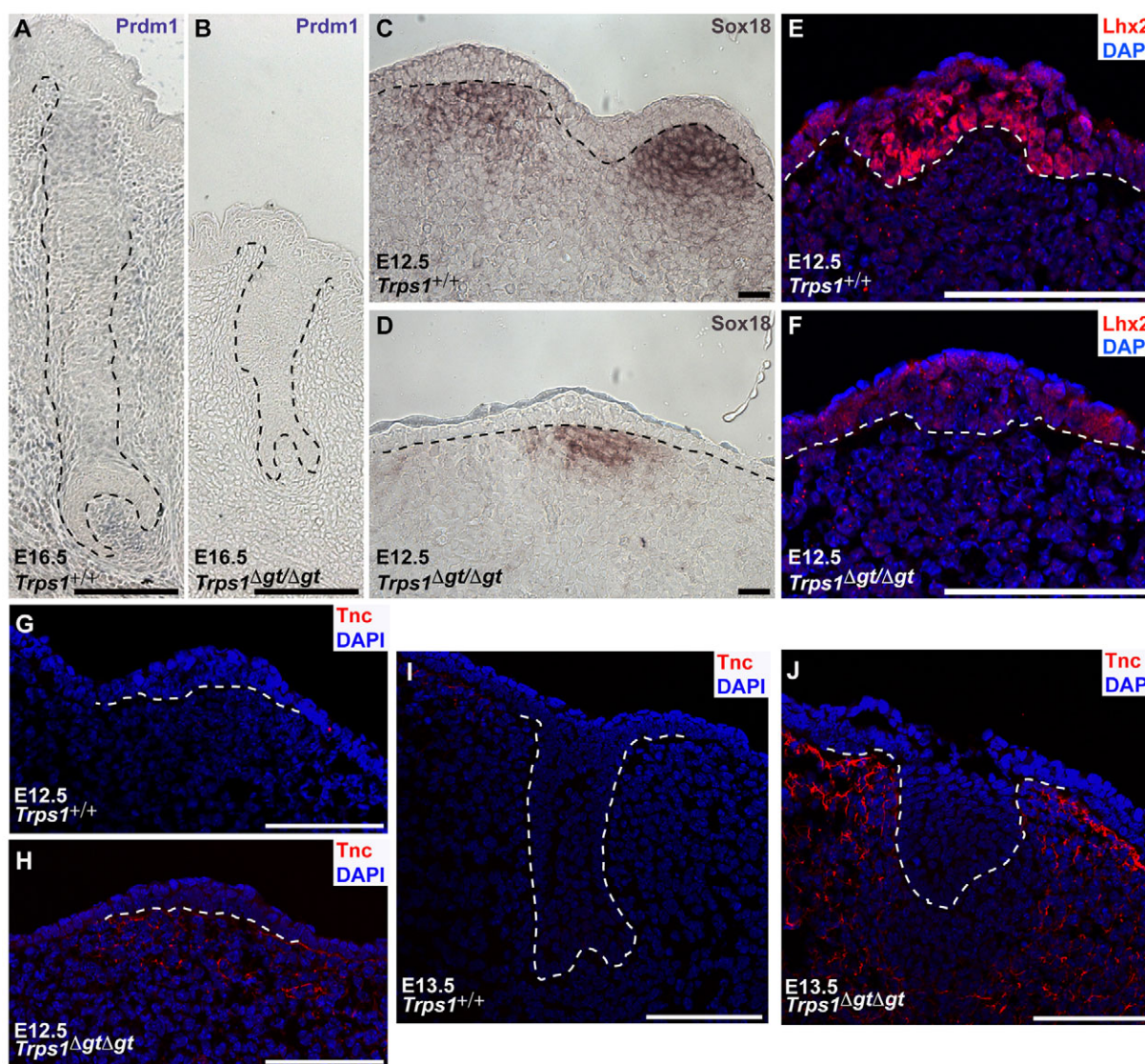
Fig. 3. Trps1 target gene expression levels are altered in vivo in *Trps1ᐞgt/ᐞgt* vibrissae follicles. (**A**,**B**) Prdm1 expression was reduced in the dermal papillae and inner root sheath precursors of *Trps1ᐞgt/ᐞgt* vibrissae at E16.5. (**C**,**D**) *Sox18* expression was reduced in the dermal condensates underlying developing vibrissae placodes in *Trps1ᐞgt/ᐞgt* embryos at E12.5. (**E**,**F**) Lhx2 staining (red) was decreased throughout the epithelial placodes of *Trps1ᐞgt/ᐞgt* vibrissae at E12.5, particularly in the basal layer. (**G-J**) Tnc staining (red) was markedly increased in the mesenchyme underlying developing *Trps1ᐞgt/ᐞgt* vibrissae at E12.5 (H) and E13.5 (J). Nuclei were stained with DAPI (blue). Dashed lines indicate basement membrane. Scale bars: 100 μm.

Sox21⁻/⁻ mice exhibit cyclic alopecia beginning at P11, resulting in a transient absence of both pelage and vibrissae follicles by P20-25 (Kiso et al., 2009). While the hair follicle phenotypes observed in *Sox21⁻/⁻* mice have a later age of onset than those observed in *Trps1ᐞgt/ᐞgt* embryos during morphogenesis, these results demonstrate a requirement for both Sox21 and Trps1 in proper vibrissa and pelage follicle maintenance.

In addition to the target genes discussed above, further examination of the lower portion of the microarray list consisting of transcripts upregulated in *Trps1ᐞgt/ᐞgt* whisker pads revealed a striking enrichment for extracellular matrix proteins and provided additional insight into the mutant phenotype. Of the transcripts associated with the proteinaceous extracellular matrix identified as potential Trps1 targets, *Egr1*, *Dcn*, *Lum*, *Tnc*, *Col8a1* and *Fus* are reportedly expressed the skin (Larsen et al., 1994; Bianco et al.,

1990; Chakravarti et al., 1995; Chiquet-Ehrismann et al., 1986; Muragaki et al., 1992; Champliaud et al., 1998). Transcripts encoding three members of the small leucine-rich proteoglycan family, *Epyc*, *Dcn* and *Lum*, were upregulated in *Trps1ᐞgt/ᐞgt* mutant whisker pads at E12.5, indicating that Trps1 may repress their expression. *Lum* has been shown to localize to the mesenchyme surrounding the developing vibrissae follicles during morphogenesis (Chakravarti, 2002). Knockout models of both *Dcn* and *Lum* are viable, with a dermal collagen defect resulting in thin, fragile skin that exhibits reduced tensile strength (Danielson et al., 1997; Chakravarti et al., 1998). The increased expression of *Epyc*, *Egr1*, *Dcn*, *Lum*, *Tnc* and *Col8a1* in *Trps1ᐞgt/ᐞgt* mutant whisker pad samples signifies defects in connective tissue assembly. Defective formation of the collagen capsules in the whisker pads of these mutant embryos may disrupt the structural stability of the
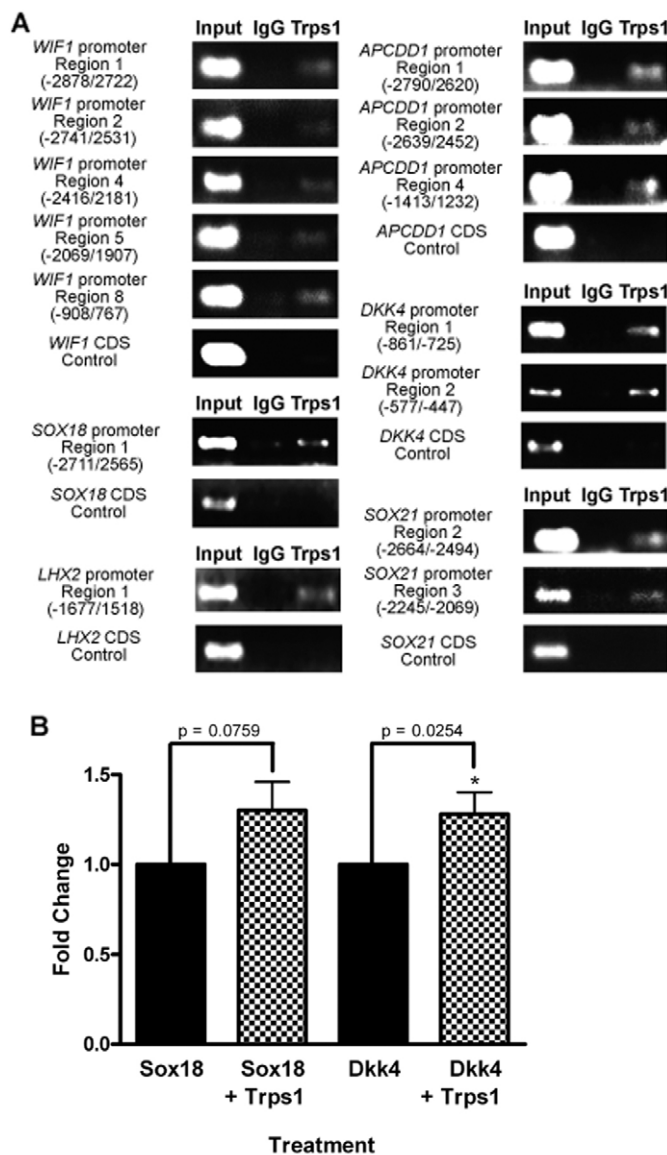
Fig. 4. Trps1 directly binds the promoters of its target genes to activate transcription. (**A**) Trps1 bound sites in the *WIF1*, *SOX18*, *LHX2*, *APCDD1*, *DKK4* and *SOX21* promoters in endogenous chromatin immunoprecipitation experiments in HEK 293T cells. No binding was observed in coding sequence (CDS)-negative control regions. (**B**) Fold changes in luciferase reporter promoter assays in Saos-2 cells demonstrating activation of *Sox18* and *Dkk4* transcription by Trps1. Statistical analyses were performed using a two-tailed unpaired *t*-test. Data are presented as mean±s.e.m. *, *P*<0.05.

developing vibrissae, perhaps contributing to the degeneration of these follicles after peg downgrowth has been initiated. Furthermore, because pelage follicles are not associated with collagen capsules, aberrant expression of these extracellular matrix proteins may in part explain the more severe phenotype observed in vibrissae follicles in $Trps1^{\Delta gt/\Delta gt}$ embryos.

Two additional transcripts of interest identified by our microarray analysis encode the transcription factor Egr1 and the extracellular matrix glycoprotein Tnc, which are expressed not only in the skin but also in the brain. *Egr1* transcript expression is significantly increased in the vibrissae-related barrel field of the

somatosensory cortex upon whisker stimulation (Patra et al., 2004). Tnc is expressed in the compact mesenchyme surrounding developing epithelia throughout the embryo, including the vibrissae follicles (Chiquet-Ehrismann et al., 1986), and, similar to *Egr1*, is also prominently expressed in various areas of the developing and adult brain, with specific expression in the vibrissae-related barrel field of the somatosensory cortex (Steindler et al., 1989; Crossin et al., 1989). Classic experiments have shown that injury of individual vibrissae results in the subsequent loss of the corresponding cortical barrel (Van der Loos and Woolsey, 1973). Notably, neuron projection (GO:0043005) was a significant GO term detected in our cellular component analysis of the transcripts upregulated in the $Trps1^{\Delta gt/\Delta gt}$ whisker pad samples (supplementary material Fig. S4). While outside the scope of the present study, the misexpression of *Egr1*, *Tnc* and several neuron projection transcripts, as well as the sparse vibrissae follicles observed in $Trps1^{\Delta gt/\Delta gt}$ mutant embryos, predict corresponding effects on the sensory function of the mystacial vibrissae and a decrease in cortical barrel density in the brain.

We have previously demonstrated that Trps1 directly represses the hair follicle stem cell specification gene *Sox9* in the follicle (our unpublished results). Interestingly, Tnc expression is significantly upregulated in both mouse (Morris et al., 2004) and human (Kloepper et al., 2008) bulge stem cell compartments, where it has been proposed to play a role in maintaining niche quiescence (Morris et al., 2004). Similarly, Lhx2 has been shown to maintain hair follicle stem cells in an undifferentiated state (Rhee et al., 2006). In combination with our previous work with *Sox9*, the finding here that Trps1 regulates the expression of both *Tnc* and *Lhx2* points to a novel role for this protein in the regulation of early hair follicle progenitors, and, potentially, adult follicle stem cells.

Of the molecules preferentially expressed in the bulge stem cell compartment of the adult follicle, Sox9 and Lhx2 are expressed earliest during follicle morphogenesis, beginning at the placode stage (Vidal et al., 2005; Rhee et al., 2006), when Sox9 is expressed in the suprabasal cells of the invaginating follicle and Lhx2 is detected in the basal layer (Nowak et al., 2008). Furthermore, they are the only known bulge markers that are additionally expressed in the bulge-derived secondary hair germ during anagen initiation (Nowak et al., 2008; Rhee et al., 2006), a site where Trps1 is also prominently expressed (Fantauzzo et al., 2008a). Using genetic marking techniques, Nowak et al. demonstrated that the early basal placode cells expressing Lhx2 are transient, whereas the suprabasal placode cells expressing Sox9 are longer lived, giving rise to the bulge stem cells and, eventually, to all the epithelial cells of the hair follicle (Nowak et al., 2008).

The differential regulation of these two transcripts by Trps1 indicates that Trps1 may be separately regulating the distinct cell populations that express these markers, both during the early stages of hair follicle morphogenesis and anagen initiation. We postulate that Trps1 activates *Lhx2* to maintain the balance of quiescence in the epithelial cells directly adjacent to the underlying dermal papilla. Consistent with this hypothesis, similar to the hair phenotype observed in $Lhx2^{-/-}$ skin grafts (Rhee et al., 2006), $Trps1^{\Delta gt/\Delta gt}$ embryos exhibit increased proliferation throughout vibrissae follicles during the hair peg stage prior to their degeneration (our unpublished results), indicating an inability to maintain cells in a state of relative quiescence.

Interestingly, our results indicate that Trps1 upregulates the expression of three Wnt inhibitors, *Wif1*, *Apcdd1* and *Dkk4*, in the vibrissa follicle and, furthermore, that this transcriptional regulation occurs through direct binding of Trps1 to the promoters of these
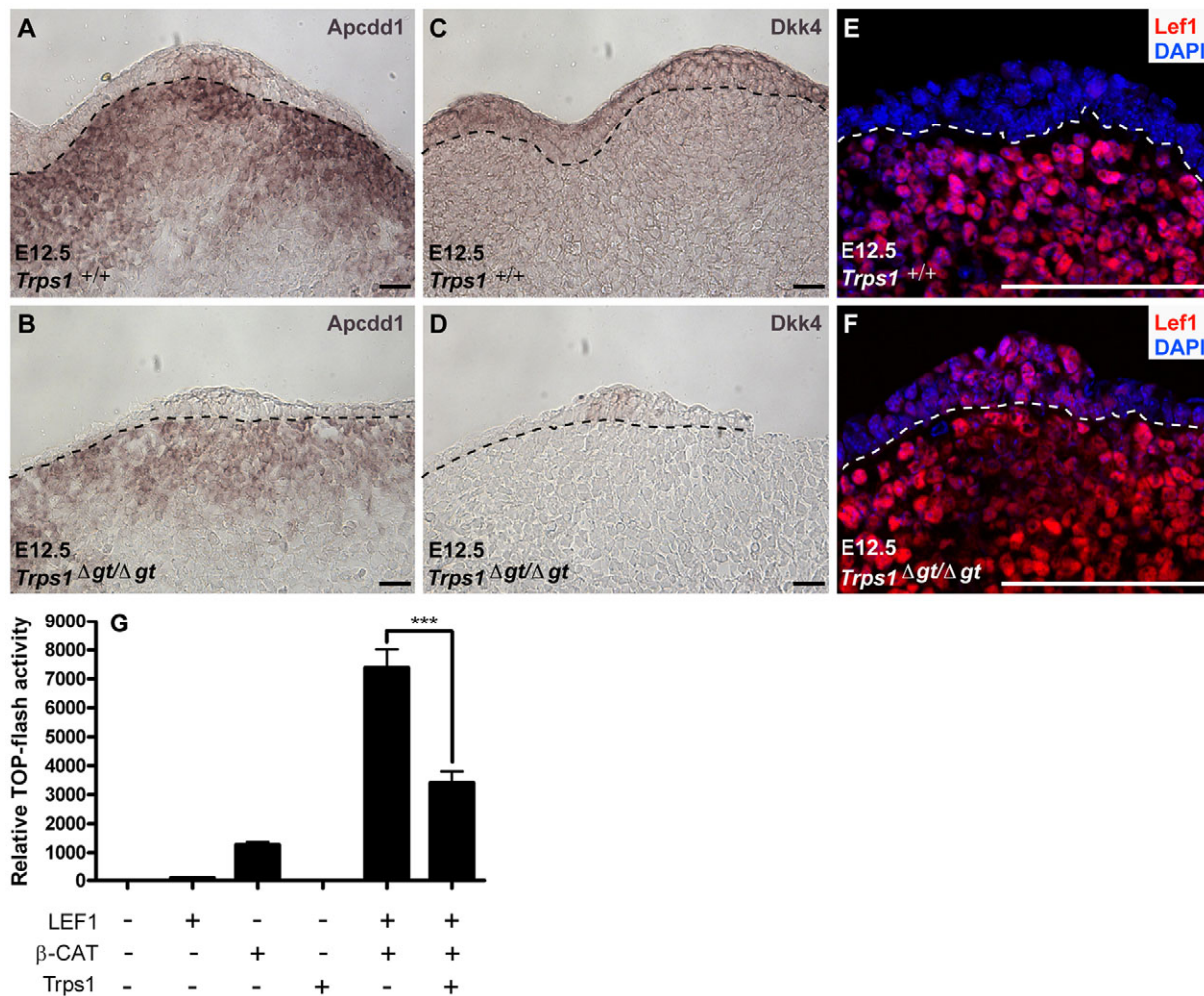
Fig. 5. Wnt expression is upregulated in $Trps1^{\Delta gt/\Delta gt}$ vibrissae follicles. (**A**,**B**) *Apcdd1* expression was decreased in the epithelial placodes and underlying mesenchyme of $Trps1^{\Delta gt/\Delta gt}$ vibrissae at E12.5. (**C**,**D**) *Dkk4* expression was reduced throughout the epithelial placodes of $Trps1^{\Delta gt/\Delta gt}$ vibrissae and the surrounding interfollicular epidermis at E12.5. (**E**,**F**) Lef1 expression (red) was markedly increased in the epithelial cells of the placodes in $Trps1^{\Delta gt/\Delta gt}$ vibrissae. Nuclei were stained with DAPI (blue). (**G**) Relative TOP-flash activity in Wnt reporter assays in HEK 293T cells demonstrating significant repression of LEF1- and β-catenin-mediated activation of TOP-flash activity upon the addition of Trps1. Statistical analyses were performed using a two-tailed unpaired *t*-test. Data are presented as mean±s.e.m. ***, $P<0.001$. Scale bars: 100 μm.

target genes. Correspondingly, we have demonstrated that the reduced expression of these Wnt inhibitors in $Trps1^{\Delta gt/\Delta gt}$ whisker pads results in an increase in Wnt signaling in the epithelial placodes of mutant vibrissae follicles. As Wnt signaling acts very early during hair follicle formation to promote the hair placode fate (Andl et al., 2002), the observation that Wnt inhibitors are dysregulated in $Trps1^{\Delta gt/\Delta gt}$ mutant whisker pads suggests that the vibrissae phenotype in these embryos might be due, in part, to disruptions in Wnt signaling during early vibrissa follicle development.

The importance of Wnt signaling in the vibrissa follicle is supported by the abnormal phenotypes observed in mice that are deficient for or overexpress members of this signaling pathway. For example, targeted disruption of *Lef1* results in the absence of vibrissae follicles (van Genderen et al., 1994), whereas transgenic overexpression of *Lef1* in the basal epidermis of the skin and hair follicle (*K14-Lef1*) leads to the development of curved, irregularly oriented vibrissae follicles in adult animals (Zhou et al., 1995). Furthermore, inhibition of Wnt signaling in the epidermis through overexpression of a *Lef1* transgene lacking the β-catenin binding

site (*K14-ΔnLef1*) results in sparse vibrissae (Niemann et al., 2002). Similarly, ablation of the effectors Tcf3/Tcf4 in the epidermis of the skin and hair follicle (*K14-Cre;Tcf3^{fl/fl};Tcf4^{−/−}*) leads to a lack of vibrissae follicles (Nguyen et al., 2009). Epidermal-specific disruption of *Ctnnb1* (*K14-Cre;Ctnnb1^{fl/fl}*), which encodes β-catenin, or overexpression of the secreted Wnt inhibitor Dkk1 in the epidermis (*K14-Dkk1*), inhibits vibrissa placode formation (Huelsken et al., 2001; Andl et al., 2002).

Both the Wnt effector Lef1 and the Wnt-responsive reporter gene *TOPGAL* are expressed in the epithelial placodes and dermal condensates of developing vibrissae follicles (van Genderen et al., 1994; DasGupta and Fuchs, 1999). Tissue recombination experiments between wild-type and *Lef1^{−/−}* embryos have demonstrated that dermal *Lef1* expression is necessary for the initiation of murine vibrissa, but not pelage, follicle formation, while epithelial *Lef1* expression is required for the completion of vibrissa follicle morphogenesis (Kratochwil et al., 1996), indicating a unique requirement for active Wnt signaling in both compartments of the developing vibrissa.

Table 2. Summary of Trps1 target genes

Gene	Function	Expression in HF and skin	Expression overlap with Trps1	Mouse model phenotype	Phenotypic overlap with Trps1$^{\Delta gt/\Delta gt}$	Trps1 binds promoter
Wif1	Secreted Wnt inhibitor	DP (Kansara et al., 2009)	Yes: DP	Null: increased osteosarcoma susceptibility (Kansara et al., 2009)	No	Yes
Prdm1	Krüppel-type zinc-finger transcription factor	DP, IRS precursors, SG, granular layer (Chang, D. H. et al., 2002)	Yes: DP, IRS precursors	cKO: defective sebocyte differentiation (Horsley et al., 2006); defective epidermal differentiation (Magnusdottir et al., 2007); absent vibrissae (Robertson et al., 2007)	Yes: absent vibrissae	No
Sox18	SRY box-containing transcription factor	Mesenchyme underlying developing follicles (Pennisi et al., 2000a)	Yes: mesenchyme underlying developing follicles	Null: reduced proportion of zigzag hairs (Pennisi et al., 2000b) *Ra*: absent vibrissae and pelage (Pennisi et al., 2000a)	Yes: absent vibrissae; reduced pelage follicle density	Yes
Lhx2	LIM homeobox transcription factor	HF placode, leading front of HG, secondary HG, bulge (Rhee et al., 2006)	Yes: epidermis at onset of HF morphogenesis, secondary HG, bulge	Tg: suppressed terminal differentiation Null: reduced pelage follicle density; premature anagen entry (Rhee et al., 2006)	Yes: reduced pelage follicle density	Yes
Apcdd1	Membrane-bound Wnt inhibitor	DP, matrix (Jukkola et al., 2004); HS (Shimomura et al., 2010)	Yes: DP, matrix, HS cuticle	nd	nd	Yes
Dkk4	Secreted Wnt inhibitor	HF placode (Bazzi et al., 2007)	Yes: epidermis at onset of HF morphogenesis	Tg: abnormal secondary follicle structure (Cui et al., 2010)	No	Yes
Sox21	SRY box-containing transcription factor	HS cuticle (Kiso et al., 2009)	Yes: HS cuticle	Null: cyclic alopecia of pelage and vibrissae follicles (Kiso et al., 2009)	Yes: reduced pelage and vibrissae follicle density	Yes

DP, dermal papilla; IRS, inner root sheath; SG, sebaceous gland; HF, hair follicle; HG, hair germ; HS, hair shaft; cKO, conditional knockout; Tg, transgenic; nd, no data available.

Similar to Lef1, Trps1 is also expressed in both compartments of the developing vibrissa follicle during embryogenesis. Subcellularly, nuclear localization of Trps1 is observed in the mesenchymal cells of the whisker pad before any histological evidence of vibrissa follicle development, signifying that Trps1 acts to alter target gene expression levels very early in the dermis. Expression of Trps1 in the nucleus of epithelial cells is observed only transiently at the onset of hair follicle morphogenesis (Fantauzzo et al., 2008a), indicating an additional role for Trps1 in the transcriptional regulation of placode formation.

These results point to a crucial role for Trps1 in both the epithelial and mesenchymal compartments of the skin at the onset of vibrissa follicle development. We propose that activation of secreted and membrane-bound Wnt inhibitors by Trps1 at the initiation of vibrissa follicle formation acts to attenuate Wnt signaling both in the epidermal placode and dermal condensate of the developing follicle, thereby allowing for proper vibrissa initiation. In *Trps1$^{\Delta gt/\Delta gt}$* whisker pads, a subset of Wnt inhibitors fail to be activated by Trps1 in the epithelial placode and dermal condensate at the initiation of vibrissa follicle morphogenesis, which is likely to contribute to defective follicle spacing and development. In support of this hypothesis, one of the Wnt inhibitors activated by Trps1, *Dkk4*, is expressed exclusively in the epithelial placodes of vibrissae and has been shown to function in negative-feedback inhibition in the hair follicle to attenuate Wnt signaling (Bazzi et al., 2007). The additional Wnt inhibitors upregulated by Trps1, *Wif1* and *Apcdd1*, are expressed in

the dermal papilla (Kansara et al., 2009; Jukkola et al., 2004) and may correspondingly mediate the effects of Trps1 in the mesenchymal compartment.

In summary, we have identified a number of transcriptional targets of Trps1 through which it regulates early vibrissa follicle organogenesis in the murine whisker pad, where, as we show for the first time, it functions not only as a transcriptional repressor but also as an activator. Notably, we have demonstrated that Trps1 orchestrates a complex morphogenetic process through subtle changes in the expression of a wide array of genes, each of which is likely to contribute in a combinatorial fashion to vibrissa development.

References
Andl, T., Reddy, S. T., Gaddapara, T. and Millar, S. E. (2002). WNT signals are required for the initiation of hair follicle development. *Dev. Cell* **2**, 643-653.
Bazzi, H., Fantauzzo, K. A., Richardson, G. D., Jahoda, C. A. and Christiano, A. M. (2007). The Wnt inhibitor, Dickkopf 4, is induced by canonical Wnt signaling during ectodermal appendage morphogenesis. *Dev. Biol.* **305**, 498-507.
Bianco, P., Fisher, L. W., Young, M. F., Termine, J. D. and Robey, P. G. (1990). Expression and localization of the two small proteoglycans biglycan and decorin in developing human skeletal and non-skeletal tissues. *J. Histochem. Cytochem.* **38**, 1549-1563.
Carter, T. C. and Phillips, R. J. S. (1954). Ragged, a semidominant coat texture mutant-in the house mouse. *J. Hered.* **45**, 150-154.
Chakravarti, S. (2002). Functions of lumican and fibromodulin: lessons from knockout mice. *Glycoconj. J.* **19**, 287-293.
Chakravarti, S., Stalling, R. L., SundarRaj, N., Cornuet, P. K. and Hassell, J. R. (1995). Primary structure of human lumican (keratan sulfate proteoglycan) and localization of the gene (LUM) to chromosome 12q21.3-q22. *Genomics* **27**, 481-488.
Chakravarti, S., Magnuson, T., Lass, J. H., Jepsen, K. J., LaMantia, C. and Carroll, H. (1998). Lumican regulates collagen fibril assembly: skin fragility and corneal opacity in the absence of lumican. *J. Cell Biol.* **141**, 1277-1286.
Champliaud, M. F., Champliaud, D., Albalat, R., Burgeson, R., Magro, C. and Baden, H. P. (1998). Localization and characterization of the RNA binding protein TLS in skin and stratified mucosa. *J. Invest. Dermatol.* **110**, 277-281.
Chang, D. H., Cattoretti, G. and Calame, K. L. (2002). The dynamic expression pattern of B lymphocyte induced maturation protein-1 (Blimp-1) during mouse embryonic development. *Mech. Dev.* **117**, 305-309.
Chang, G. T., van den Bemd, G. J., Jhamai, M. and Brinkmann, A. O. (2002). Structure and function of GC79/TRPS1, a novel androgen-repressible apoptosis gene. *Apoptosis* **7**, 13-21.
Chiquet-Ehrismann, R., Mackie, E. J., Pearson, C. A. and Sakakura, T. (1986). Tenascin: an extracellular matrix protein involved in tissue interactions during fetal development and oncogenesis. *Cell* **47**, 131-139.
Crossin, K. L., Hoffman, S., Tan, S. S. and Edelman, G. M. (1989). Cytotactin and its proteoglycan ligand mark structural and functional boundaries in somatosensory cortex of the early postnatal mouse. *Dev. Biol.* **136**, 381-392.
Cui, C. Y., Kunisada, M., Piao, Y., Childress, V., Ko, M. S. and Schlessinger, D. (2010). Dkk4 and Eda regulate distinctive developmental mechanisms for subtypes of mouse hair. *PLoS ONE* **5**, e10009.
Danielson, K. G., Baribault, H., Holmes, D. F., Graham, H., Kadler, K. E. and Iozzo, R. V. (1997). Targeted disruption of decorin leads to abnormal collagen fibril morphology and skin fragility. *J. Cell Biol.* **136**, 729-743.
DasGupta, R. and Fuchs, E. (1999). Multiple roles for activated LEF/TCF transcription complexes during hair follicle development and differentiation. *Development* **126**, 4557-4568.
Fantauzzo, K. A., Bazzi, H., Jahoda, C. A. and Christiano, A. M. (2008a). Dynamic expression of the zinc-finger transcription factor Trps1 during hair follicle morphogenesis and cycling. *Gene Expr. Patterns* **8**, 51-57.
Fantauzzo, K. A., Tadin-Strapps, M., You, Y., Mentzer, S. E., Baumeister, F. A., Cianfarani, S., Van Maldergem, L., Warburton, D., Sundberg, J. P. and Christiano, A. M. (2008b). A position effect on TRPS1 is associated with Ambras syndrome in humans and the Koala phenotype in mice. *Hum. Mol. Genet.* **17**, 3539-3551.
Giedion, A., Burdea, M., Fruchter, Z., Meloni, T. and Trosc, V. (1973). Autosomal-dominant transmission of the tricho-rhino-phalangeal syndrome. Report of 4 unrelated families, review of 60 cases. *Helv. Paediatr. Acta* **28**, 249-259.
Hilton, M. J., Sawyer, J. M., Gutierrez, L., Hogart, A., Kung, T. C. and Wells, D. E. (2002). Analysis of novel and recurrent mutations responsible for the tricho-rhino-phalangeal syndromes. *J. Hum. Genet.* **47**, 103-106.
Horsley, V., O'Carroll, D., Tooze, R., Ohinata, Y., Saitou, M., Obukhanych, T., Nussenzweig, M., Tarakhovsky, A. and Fuchs, E. (2006). Blimp1 defines a progenitor population that governs cellular input to the sebaceous gland. *Cell* **126**, 597-609.
Huelsken, J., Vogel, R., Erdmann, B., Cotsarelis, G. and Birchmeier, W. (2001). beta-Catenin controls hair follicle morphogenesis and stem cell differentiation in the skin. *Cell* **105**, 533-545.

Irrthum, A., Devriendt, K., Chitayat, D., Matthijs, G., Glade, C., Steijlen, P. M., Fryns, J. P., Van Steensel, M. A. and Vikkula, M. (2003). Mutations in the transcription factor gene SOX18 underlie recessive and dominant forms of hypotrichosis-lymphedema-telangiectasia. *Am. J. Hum. Genet.* **72**, 1470-1478.
Jukkola, T., Sinjushina, N. and Partanen, J. (2004). Drapc1 expression during mouse embryonic development. *Gene Expr. Patterns* **4**, 755-762.
Kaiser, F. J., Brega, P., Raff, M. L., Byers, P. H., Gallati, S., Kay, T. T., de Almeida, S., Horsthemke, B. and Ludecke, H. J. (2004). Novel missense mutations in the TRPS1 transcription factor define the nuclear localization signal. *Eur. J. Hum. Genet.* **12**, 121-126.
Kansara, M., Tsang, M., Kodjabachian, L., Sims, N. A., Trivett, M. K., Ehrich, M., Dobrovic, A., Slavin, J., Choong, P. F., Simmons, P. J. et al. (2009). Wnt inhibitory factor 1 is epigenetically silenced in human osteosarcoma, and targeted disruption accelerates osteosarcomagenesis in mice. *J. Clin. Invest.* **119**, 837-851.
Kiso, M., Tanaka, S., Saba, R., Matsuda, S., Shimizu, A., Ohyama, M., Okano, H. J., Shiroishi, T., Okano, H. and Saga, Y. (2009). The disruption of Sox21-mediated hair shaft cuticle differentiation causes cyclic alopecia in mice. *Proc. Natl. Acad. Sci. USA* **106**, 9292-9297.
Kloepper, J. E., Tiede, S., Brinckmann, J., Reinhardt, D. P., Meyer, W., Faessler, R. and Paus, R. (2008). Immunophenotyping of the human bulge region: the quest to define useful in situ markers for human epithelial hair follicle stem cells and their niche. *Exp. Dermatol.* **17**, 592-609.
Kobayashi, H., Hino, M., Shimodahira, M., Iwakura, T., Ishihara, T., Ikekubo, K., Ogawa, Y., Nakao, K. and Kurahachi, H. (2002). Missense mutation of TRPS1 in a family of tricho-rhino-phalangeal syndrome type III. *Am. J. Med. Genet.* **107**, 26-29.
Kratochwil, K., Dull, M., Farinas, I., Galceran, J. and Grosschedl, R. (1996). Lef1 expression is activated by BMP-4 and regulates inductive tissue interactions in tooth and hair development. *Genes Dev.* **10**, 1382-1394.
Larsen, F. G., Voorhees, J. J. and Aström, A. (1994). Retinoic acid induces expression of early growth response gene-1 (Egr-1) in human skin in vivo and in cultured skin fibroblasts. *J. Invest. Dermatol.* **102**, 730-733.
Ludecke, H. J., Schaper, J., Meinecke, P., Momeni, P., Gross, S., von Holtum, D., Hirche, H., Abramowicz, M. J., Albrecht, B., Apacik, C. et al. (2001). Genotypic and phenotypic spectrum in tricho-rhino-phalangeal syndrome types I and III. *Am. J. Hum. Genet.* **68**, 81-91.
Magnusdottir, E., Kalachikov, S., Mizukoshi, K., Savitsky, D., Ishida-Yamamoto, A., Panteleyev, A. A. and Calame, K. (2007). Epidermal terminal differentiation depends on B lymphocyte-induced maturation protein-1. *Proc. Natl. Acad. Sci. USA* **104**, 14988-14993.
Malik, T. H., Shoichet, S. A., Latham, P., Kroll, T. G., Peters, L. L. and Shivdasani, R. A. (2001). Transcriptional repression and developmental functions of the atypical vertebrate GATA protein TRPS1. *EMBO J.* **20**, 1715-1725.
Malik, T. H., Von Stechow, D., Bronson, R. T. and Shivdasani, R. A. (2002). Deletion of the GATA domain of TRPS1 causes an absence of facial hair and provides new insights into the bone disorder in inherited tricho-rhino-phalangeal syndromes. *Mol. Cell. Biol.* **22**, 8592-8600.
Momeni, P., Glockner, G., Schmidt, O., von Holtum, D., Albrecht, B., Gillessen-Kaesbach, G., Hennekam, R., Meinecke, P., Zabel, B., Rosenthal, A. et al. (2000). Mutations in a new gene, encoding a zinc-finger protein, cause tricho-rhino-phalangeal syndrome type I. *Nat. Genet.* **24**, 71-74.
Morris, R. J., Liu, Y., Marles, L., Yang, Z., Trempus, C., Li, S., Lin, J. S., Sawicki, J. A. and Cotsarelis, G. (2004). Capturing and profiling adult hair follicle stem cells. *Nat. Biotechnol.* **22**, 411-417.
Muragaki, Y., Shiota, C., Inoue, M., Ooshima, A., Olsen, B. R. and Ninomiya, Y. (1992). alpha 1 (VIII)-collagen gene transcripts encode a short-chain collagen polypeptide and are expressed by various epithelial, endothelial and mesenchymal cells in newborn mouse tissues. *Eur. J. Biochem.* **207**, 895-902.
Napierala, D., Garcia-Rojas, X., Sam, K., Wakui, K., Chen, C., Mendoza-Londono, R., Zhou, G., Zheng, Q. and Lee, B. (2005). Mutations and promoter SNPs in RUNX2, a transcriptional regulator of bone formation. *Mol. Genet. Metab.* **86**, 257-268.
Nguyen, H., Merrill, B. J., Polak, L., Nikolova, M., Rendl, M., Shaver, T. M., Pasolli, H. A. and Fuchs, E. (2009). Tcf3 and Tcf4 are essential for long-term homeostasis of skin epithelia. *Nat. Genet.* **41**, 1068-1075.
Niemann, C., Owens, D. M., Hulsken, J., Birchmeier, W. and Watt, F. M. (2002). Expression of DeltaNLef1 in mouse epidermis results in differentiation of hair follicles into squamous epidermal cysts and formation of skin tumours. *Development* **129**, 95-109.
Nishioka, K., Itoh, S., Suemoto, H., Kanno, S., Gai, Z., Kawakatsu, M., Tanishima, H., Morimoto, Y., Hatamura, I., Yoshida, M. et al. (2008). Trps1 deficiency enlarges the proliferative zone of growth plate cartilage by upregulation of Pthrp. *Bone* **43**, 64-71.
Nowak, J. A., Polak, L., Pasolli, H. A. and Fuchs, E. (2008). Hair follicle stem cells are specified and function in early skin morphogenesis. *Cell Stem Cell* **3**, 33-43.

DEVELOPMENT

Patra, R. C., Blue, M. E., Johnston, M. V., Bressler, J. and Wilson, M. A. (2004). Activity-dependent expression of Egr1 mRNA in somatosensory cortex of developing rats. *J. Neurosci. Res.* **78**, 235-244.

Pennisi, D., Gardner, J., Chambers, D., Hosking, B., Peters, J., Muscat, G., Abbott, C. and Koopman, P. (2000a). Mutations in Sox18 underlie cardiovascular and hair follicle defects in ragged mice. *Nat. Genet.* **24**, 434-437.

Pennisi, D., Bowles, J., Nagy, A., Muscat, G. and Koopman, P. (2000b). Mice null for sox18 are viable and display a mild coat defect. *Mol. Cell. Biol.* **20**, 9331-9336.

Piccione, M., Niceta, M., Antona, V., Di Fiore, A., Cariola, F., Gentile, M. and Corsello, G. (2009). Identification of two new mutations in TRPS 1 gene leading to the tricho-rhino-phalangeal syndrome type I and III. *Am. J. Med. Genet. A* **149**, 1837-1841.

Piscopo, D. M., Johansen, E. B. and Derynck, R. (2009). Identification of the GATA factor TRPS1 as a repressor of the osteocalcin promoter. *J. Biol. Chem.* **284**, 31690-31703.

Rhee, H., Polak, L. and Fuchs, E. (2006). Lhx2 maintains stem cell character in hair follicles. *Science* **312**, 1946-1949.

Robertson, E. J., Charatsi, I., Joyner, C. J., Koonce, C. H., Morgan, M., Islam, A., Paterson, C., Lejsek, E., Arnold, S. J., Kallies, A. et al. (2007). Blimp1 regulates development of the posterior forelimb, caudal pharyngeal arches, heart and sensory vibrissae in mice. *Development* **134**, 4335-4345.

Rossi, A., Devirgiliis, V., Panasiti, V., Borroni, R. G., Carlesimo, M., Gentile, M., Cariola, F. and Calvieri, S. (2007). Missense mutation in exon 7 of TRPS1 gene in an Italian family with a mild form of trichorhinophalangeal syndrome type I. *Br. J. Dermatol.* **157**, 1021-1024.

Seitz, C. S., Ludecke, H. J., Wagner, N., Brocker, E. B. and Hamm, H. (2001). Trichorhinophalangeal syndrome type I: clinical and molecular characterization of 3 members of a family and 1 sporadic case. *Arch. Dermatol.* **137**, 1437-1442.

Shimomura, Y., Agalliu, D., Vonica, A., Luria, V., Wajid, M., Baumer, A., Belli, S., Petukhova, L., Schinzel, A., Brivanlou, A. H. et al. (2010). APCDD1 is a novel Wnt inhibitor mutated in hereditary hypotrichosis simplex. *Nature* **464**, 1043-1047.

Steindler, D. A., Cooper, N. G., Faissner, A. and Schachner, M. (1989). Boundaries defined by adhesion molecules during development of the cerebral cortex: the J1/tenascin glycoprotein in the mouse somatosensory cortical barrel field. *Dev. Biol.* **131**, 243-260.

Suemoto, H., Muragaki, Y., Nishioka, K., Sato, M., Ooshima, A., Itoh, S., Hatamura, I., Ozaki, M., Braun, A., Gustafsson, E. et al. (2007). Trps1 regulates proliferation and apoptosis of chondrocytes through Stat3 signaling. *Dev. Biol.* **312**, 572-581.

Törnqvist, G., Sandberg, A., Hägglund, A. C. and Carlsson, L. (2010). Cyclic expression of lhx2 regulates hair formation. *PLoS Genet.* **6**, e1000904.

van den Bemd, G. J., Jhamai, M., Brinkmann, A. O. and Chang, G. T. (2003). The atypical GATA protein TRPS1 represses androgen-induced prostate-specific antigen expression in LNCaP prostate cancer cells. *Biochem. Biophys. Res. Commun.* **312**, 578-584.

Van der Loos, H. and Woolsey, T. A. (1973). Somatosensory cortex: structural alterations following early injury to sense organs. *Science* **179**, 395-398.

van Genderen, C., Okamura, R. M., Farinas, I., Quo, R. G., Parslow, T. G., Bruhn, L. and Grosschedl, R. (1994). Development of several organs that require inductive epithelial-mesenchymal interactions is impaired in LEF-1-deficient mice. *Genes Dev.* **8**, 2691-2703.

Vidal, V. P., Chaboissier, M. C., Lutzkendorf, S., Cotsarelis, G., Mill, P., Hui, C. C., Ortonne, N., Ortonne, J. P. and Schedl, A. (2005). Sox9 is essential for outer root sheath differentiation and the formation of the hair stem cell compartment. *Curr. Biol.* **15**, 1340-1351.

Zhou, P., Byrne, C., Jacobs, J. and Fuchs, E. (1995). Lymphoid enhancer factor 1 directs hair follicle patterning and epithelial cell fate. *Genes Dev.* **9**, 700-713.

Table S1. Primers used in qRT-PCR and ChIP analyses

qRT-PCR

Transcript (mouse)	Forward primer (5′ to 3′)	Reverse primer (5′ to 3′)
B2m	ACTGACCGGCCTGTATGCTA	TGAAGGACATATCTGACATCTCTA
Wif1	CAAAGAATGCCAGCCATTCC	CAGCAAAGGGACATTGACAG
Prdm1	CTGCCAACAACAGCAAAGAG	GGAACTCCTCTCTGGAATAG
Sox18	GAAGAGAGCAGCCTCATTTC	CATATGCGAAAGGAAGGGAG
Lhx2	CAGATCTGGCAGCTTACAAC	CTGCTTCAAGTCCTTGGCAT
Apcdd1	CTACCCAGAGGGTGTTCTAC	CAATGGTCAGGTCAGCCTTG
Dkk4	CTGTGTGAATGATGTTTGCAC	GTCAGAGGTTCTAAGACAGC
Sox21	GATGTATAGGTGTCAGGCAG	GCAAAGCAAACACCAACTGC
Epyc	GTATGATGCCATCTTGGAGG	CCTTGTCTTCATCCTGGTTG
Calb1	GTGGTTACCTGGAAGGAAAG	GCATCGAAAGAGCAGCAAGA
Dcn	CAAGAACCTGAAGGACTTGC	GAAGTTCCTGGAGAGTTCTG
Lum	CCTGGAGGTCAATGAACTTG	CACTCATACATGTCAGGAGG
Tnc	CAAAACCATCAGTACCACGG	GGAGGGATATTTCTTGTGGC

ChIP

Region (human)	Position relative to exon 1	Forward primer (5′ to 3′)	Reverse primer (5′ to 3′)
WIF1 pR1	−2878 to −2722	agttgacttgcctagcacat	gaatcaggcttgactctcct
WIF1 pR2	−2741 to −2531	aggagagtcaagcctgattc	tccagcacaggacacttaga
WIF1 pR3	−2550 to −2397	tctaagtgtcctgtgctgga	ttctctcctaactcggtttc
WIF1 pR4	−2416 to −2181	gaaaccgagttaggagagaa	ataatgccagtgtcacccag
WIF1 pR5	−2069 to −1907	aggaagaatcactgtgaagc	ccagtaagttgactgtggat
WIF1 pR6	−1895 to −1709	cctctttcctcgtcagtaaa	ttgcagctatacaaccaacc
WIF1 pR7	−1220 to −1060	tttttttgagacggagtctcg	gcaaaaattagctgggcatg
WIF1 pR8	−908 to −767	cagcaaacgtgaagatatcc	acacccagcatttgggggatt
WIF1 pR9	−194 to +47	cttcccgctcttctgttct	agggctgttcccgtttaga
WIF1 CDS	Exon 4	GTTCAAGTTGGTTTCCCATG	GCATTTTGAGGTGTTTGGAG
SOX18 pR1	−2711 to −2565	aactctgcctttctgactgg	aaaagagggcaggcagttca
SOX18 CDS	Exon 2	ACGCGTGTATGTTTGGTTCC	ATGTAACCCTGGCAACTCT
LHX2 pR1	−1677 to −1518	caagtgcaggtataacgtgc	caataacacagccagcacga
LHX2 CDS	Exon 4	AACGAAAACGACGCAGAGCA	TGCTTCAAGTCCTTGGCGT
APCDD1 pR1	−2790 to −2620	tcctcttctccatcagcatg	ttacgagaacccaagcctca
APCDD1 pR2	−2639 to −2452	tgaggcttgggttctcgtaa	gaaaggaaaaggaagacatg
APCDD1 pR3	−1567 to −1394	gatttgcaaacaggagcaca	acctgagaaatccatgggtg
APCDD1 pR4	−1413 to −1232	cacccatggatttctcaggt	aatgcctgatttcccaagag
APCDD1 CDS	Exon 2	TTCATCCAGACAGCAGGTCT	CTCGATTGTAGGTGGCATCT
DKK4 pR1	−861 to −725	gacttggatccttgttctgc	ccattttcaatggtgggaac
DKK4 pR2	−577 to −447	tggatgccagagctaatcag	tggccaatatgctatagagg
DKK4 CDS	Exon 3	CTACGATGGAAGATGCAACC	CCTTCCTGCCTTGTGATTTC
SOX21 pR1	−2921 to −2760	taggtgaaaagctcagggac	ccatattcctttacaggctc
SOX21 pR2	−2664 to −2494	cacatagatgccactgctgt	cacacacacacacaaaagct
SOX21 pR3	−2245 to −2069	gctgtttgacttctgcatcg	ctgctgaggtgaaggtgttt
SOX21 pR4	−2088 to −1920	aaacaccttcacctcagcag	ccagactgagagtatgcatc
SOX21 CDS	Exon 1	ACAACTCGGAGATCAGCAAG	CGAACTTGTCCTTCTTGAGC